A Numerical Study on the Triboelectrostatic Separation of PVC Materials From Mixed Plastics for Waste Plastic Recycling

Man Yeong Ha*, Chung Hwan Jeon, Doo Seong Choi
School of Mechnaical Engineering, Pusan National University, San 30 Jangjeon-dong, Kumjung-ku, Pusan 609-735, Korea
Hae-Jin Choi
KARI, Youseong, Daejeon 305-333, Korea

We investigate the triboelectrostatic separation of polyvinylchloride (PVC) from mixed plastics in the laborartory scale triboelectrostatic separation system. The flow and electric fields in the precipitator are obtained from the numerical solution of finite volume method. Using these flow and electric fields, we solved the particle motion equation considering the inertia, drag, gravity and electrostatic forces acted on the particles. The particle trajectories are obtained using a Lagrangian method as a function of different important variables such as Reynolds number, Stokes number, electrostatic force, electric charge and electric field distribution, inclined angle of plane electrodes, particle rebounding, particle charge decay rate after impact on the electrode surface, etc., in order to determine the optimal design conditions. The present predicted results for the cumulative yield represent well the experimental ones.

Key Words : Electrostatic Separation, Waste Plastic Separation, Yield, Numerical Simulation

1. Introduction

The electrostatic separation method is to separate the mixed particles with different electric properties by using the electrostatic force. In this study, we investigate the separation characteristics of mixed waste plastic particles. Recycling of waste plastic materials is very important because it prevents the environmental pollution and recycled plastics can be reused as industrial ingredients. The raw materials and products of plastics are very widely used in our daily life and industries. However, if the plastics are left in the environment without any controls, they can cause very serious pollution problems to the environment. Thus the recycling of waste plastics is required to prevent the pollution problems due to waste plastics. However, because the plastics are the mixture of different chemical components, it is not easy to classify different chemical components directly into orders by hands. In order to apply the electrostatic separation technique, the waste plastics are first converted into powder using the mill. This powder is electrically charged by friction in the tribocharger, which has different types of spiral tube, fluidized bed, rotational cylinder, etc. The electric characteristics of charged particles depend on the chemical components to consist of the waste plastics. If we apply the electrostatic force to the differentially charged particles, we can easily classify the particles into orders with the same chemical components.

Recently, a dry triboelectrostatic process has been considered to apply to recycle waste plastics. This process is useful to separate PVC from the mixed plastics, which is based on the difference in the surface charge of various components of the powder mixture by the particle-to-particle impact and the particle-to-wall impact. Some of

* Corresponding Author,
E-mail : myha@pusan.ac.kr
TEL : +82-51-510-2440; **FAX** : +82-51-512-9835
School of Mechnaical Engineering, Pusan National University, San 30 Jangjeon-dong, Kumjung-ku, Pusan 609-735, Korea. (Manuscript **Received** March 25, 2003; **Revised** May 29, 2003)

the mechanism proposed for electrostatic contact charging is electron transitions between the materials coming into contact and ion exchange (Harper, 1967). In a practical application of triboelectrification for plastic recycling, many researchers have been studying the separation experiments of various plastics using the tribocharger such as a cyclone (Pearse. and Hickey, 1978; Yanar and Kwetkus, 1995) a rotary blade (Matsushita et al., 1999), and a rotating tube (Inculet et al, 1994). Also, Kang et al.(1999), Lu et al.(1999) and Takeshita et al.(1998) have investigated the particle flow behavior and the stability of operation of a perforated plate type suspension bed in three-phase fluidized beds, respectively. Due to the inherent complexity of phenomena in the electrostatic particle separation, the experimental study shows mainly the separation efficiency as a function of related important variables such as fluid flow rate, separator geometry, the type of tribocharger, the electric charge amount of particles, applied voltage difference, etc. The physics related with particle separation in the presence of electric fields are very complex, and the separation efficiency depends on the interaction of many related variables, such as the flow and electric fields in the separator, the rate of particle loading, the electric charge distribution of particles, the interaction between the turbulent flow and particle motion, the geometry of electric separator, etc. In order to know the detail physics related to the electrostatic particle separation and its effect on the performance on the separator, some theoretical studies are carried out using the simple and complex flow models. Chen et al.(1993) calculated the particle trajectory and deposition in the convergent and parallel channel. They considered the uniform and developing laminar flow with a dilute particle concentration in the presence of electric fields. The effect of relative size of drag, gravity and electrostatic force term on the particle deposition is investigated using the simple laminar flow. Ashano et al.(1996) investigated the trajectory of charged metal particles (about 1 mm size) in a gas-insulated switchgear in the parallel and tilted electrodes. They obtained the theoretical solution for the particle trajectory using the drag force under the simple Stokes flow assumption. The theoretical results were compared with experimental ones and showed reasonably good agreement between them. Goo and Lee (1996) obtained the deposition of charged particles in a plate-plate electrostatic precipitator. They carried out the Lagrangian method using Monte-Carlo simulation which uses the concept of time series analysis for the particle motion in a fully developed turbulent flow. The collection efficiencies are obtained as a function of Peclet number and Deutsch number. Soltani et al.(1998) studied wall deposition of charged particle in a turbulent channel flow in the presence of electrostatic charges. The turbulent flow velocity field was generated by a direct numerical simulation. Effects of particle size and electric field intensity on particle dispersion and wall deposition rate were investigated.

In the present study, we investigate the trajectory of waste plastic particles in the range of 0.5~2 mm size and their separation characteristics in the bench scale electrostatic precipitator (ESP). The flow and electric fields in the precipitator are obtained from the numerical solution. Using these flow and electric fields, we calculated the drag, gravity and electrostatic forces acted on the particles and obtained particle trajectories as a function of different important variables, in order to determine the optimal design conditions.

2. Mathematical Model

Figure 1 shows the geometry of electrostatic precipitator (ESP) used in the present calculation. The inlet and four sides of the present ESP are covered by the flat plate. The inlet has a hole to inject waste plastic particles with air. The outlet is exposed to the atmosphere. The collector containing five collection bins is placed at the bottom of the separation chamber to catch the particles escaping the outlet. The bins closely located to the positive high voltage electrode collect the negatively charged material, while the opposite side bins collect the positive charged

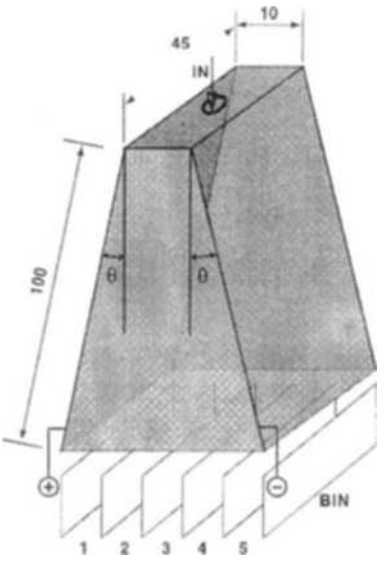

Fig. 1 Schematic diagram of electrostatic separation system used in the present calculation

material. We investigated the effect of ESP geometry on the particle trajectory and separation efficiency by considering the different angles of plane electrodes at $\theta=0°$, 2.5° and 5°. The mass and momentum conservation equations to govern the fluid flow in the ESP are defined as

$$\frac{\partial u_i}{\partial x_i}=0 \tag{1}$$

$$\frac{\partial}{\partial x_j}(u_i u_j) = \frac{1}{\mathrm{Re}}\frac{\partial}{\partial x_j}\left[\left(\frac{\partial u_i}{\partial x_j}+\frac{\partial u_j}{\partial x_i}\right)-\left(\frac{2}{3}\frac{\partial u_l}{\partial x_l}\right)\right]-\frac{\partial p}{\partial x_i} \tag{2}$$

The dimensionless variables in the above equations are defined as

$$x_i=\frac{x_i^*}{H},\ u_i=\frac{u_i^*}{U},\ p=\frac{p^*}{\rho U^2} \tag{3}$$

In the above equations, ρ, U and H represent the density, inlet velocity through the inlet hole and half height between the plane electrodes at the inlet, respectively. The superscript * in Eq. (3) represent the dimensional variable. u_i and p are the non-dimensional velocity and pressure. The above non-dimensionalization gives an important dimensionless parameter of Reynolds number

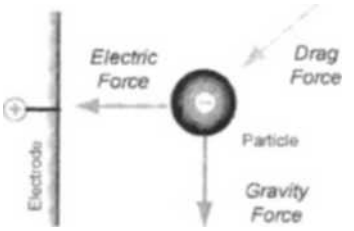

Fig. 2 Schematic diagram to show the forces acted on the negatively charged particle

($\mathrm{Re}=\frac{\rho UH}{\mu}$, where μ is the viscosity). These governing equations are solved by the numerical solution of finite volume method (Patankar, 1980).

The trajectory of negatively charged particles injected through the hole at the inlet of ESP with air is calculated by the Lagrangian method. We considered the viscous drag, gravity and electrostatic forces acted on the particle as shown in Figure 2 and the resulting equation of particle motion is defined as

$$\frac{du_i^p}{dt}=\frac{1}{24}\frac{\mathrm{Re}C_D}{St}\,|u_i-u_i^p|(u_i-u_i^p)+G_i+Q_i \tag{4}$$

Here the dimensionless variables are defined as

$$t=\frac{t^*U}{H},\ u_i^p=\frac{u_i^{p^*}}{U},\ St=\frac{\rho_p d_p^2 U}{18\mu H},\quad G_i=\frac{g_i H}{U^2},\ Q_i=\frac{qE_i H}{m_p U^2} \tag{5}$$

In the above equations, t and t^* are non-dimensional and dimensional time. u_i^p and $u_i^{p^*}$ are non-dimensional and dimensional i-directional particle velocity. ρ_p, d_p, g_i, q and E_i are particle density, particle diameter, i-directional gravity, average value of particle charge distribution and i-directional electric field. G and Q in Eq. (5) represent the dimensionless variables for the gravity and electric fields. St is the Stokes number. The first, second and third terms of right hand side in Eq. (4) represent the drag, gravity and electrostatic forces acted on the moving particle, respectively. Because the particle size considered in the present study is relatively large in the range of 0.5 mm~2 mm, the effects of added mass, pressure gradient, history and lift

forces are neglected. The drag coefficient C_D in Eq. (4) is expressed as

$$\begin{aligned} C_D &= \frac{24}{\mathrm{Re}_p}, && \mathrm{Re}_p < 0.1 \\ &= \frac{24}{\mathrm{Re}_p}(1+0.0916\mathrm{Re}_p), && 0.1 \le \mathrm{Re}_p < 5 \\ &= \frac{24}{\mathrm{Re}_p}(1+0.158\mathrm{Re}_p^{2/3}), && 5 \le \mathrm{Re}_p < 1000 \\ &= 0.44, && 1000 \le \mathrm{Re}_p \end{aligned} \tag{6}$$

where Re_p is the particle Reynolds number defined as

$$\mathrm{Re}_p = \frac{|u_i^* - u_i^p| d_p}{\nu} \tag{7}$$

where ν is the dynamic viscosity. The particle trajectory is obtained by solving the following equation using the particle velocity obtained from the solution of particle motion Eq. (4).

$$\frac{dx_i^p}{dt} = u_i^p \tag{8}$$

where x_i^p is the particle trajectory. The third order Adams-Bashforth method is used for the numerical solution of Eq. (4) and (8).

In order to calculate the electrostatic force acted on the charged particle, we should determine the distribution of electric fields E_i in Eq. (4). If the plane electrodes are parallel with $\theta=0$, the electric fields between two parallel plates are constant defined as

$$E_x = E_z = 0, \quad E_y = \frac{\Delta V}{2H} \tag{9}$$

where ΔV is the voltage difference between two parallel electrodes. However, if the plane electrodes are inclined with $\theta=2.5$ and 5.0 as shown in Fig. 1, the electric fields are not uniform in the ESP but obtained by the solution of the following equation defined as

$$E_i = -\frac{\partial \phi}{\partial x_i} \tag{10}$$

where ϕ is the electric potential obtained from the solution of the following equation defined as

$$\frac{\partial^2 \phi}{\partial x_i \partial x_i} = 0 \tag{11}$$

The governing Eq. (9) and (10) are defined in the generalized coordinate system to consider the geometry of the inclined ESP and solved by the finite volume method, similar to the numerical solution of mass and momentum conservation Eq. (1) and (2).

3. Results and Discussion

Figure 3 shows the grid system used in the present calculation. The number of grid used is $73\times65\times51$ in the x-, y-, and z-directions, respectively. Figure 4 shows x-directional (streamwise) velocity contour and velocity vectors for different inclined angles of $\theta=0°$, 0.25° and 0.50° at Re=1397, corresponding to $U=0.5$ m/s and $H=0.05$ m.

The fluid flow close to the inlet of ESP shows the typical pattern of jet flow. The jet emerges from the small inlet hole and mixes with the surrounding fluid. The emerging jet carries with it some of surrounding fluid which was originally at rest. The jet spreads outwards in the downstream direction owing to the influence of friction, whereas its velocity at the center decreases in the same direction. The fluid flow changes its pattern from the jet flow to the channel flow at the parallel or diverging channel, as the flow moves from the inlet to the outlet of the ESP. The velocity magnitude in the ESP decreases with increasing θ, because the cross sectional area in the streamwise direction increases.

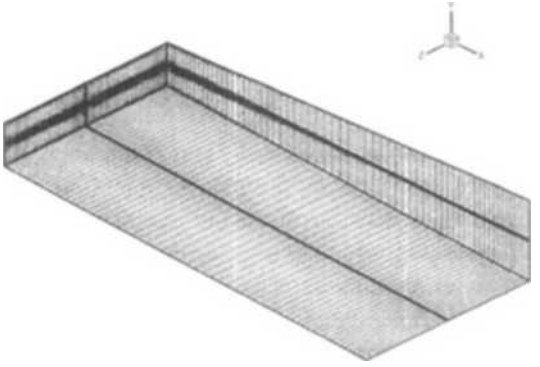

Fig. 3 Grid system used in the present calculation

Figure 5 shows the y-directional electric field E_y at the centerline of $y=0$ as a function of dimensionless distance x for different electrode angles and applied voltage differences. If the electrodes are parallel with $\theta=0$, E_y is constant as given in Eq. (8). However, if the electrodes are inclined with increasing θ, the distance between the plane electrodes increases, resulting in the

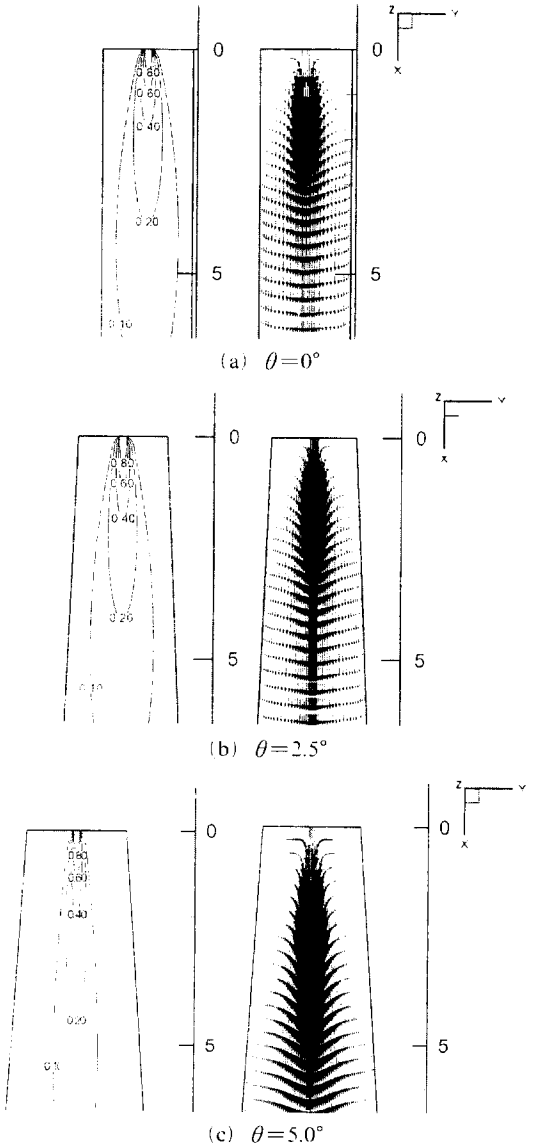

(a) $\theta=0°$

(b) $\theta=2.5°$

(c) $\theta=5.0°$

Fig. 4 x-directional velocity contours and velocity vector for different electrode angles of $\theta=0°$, 2.5° and 5.0° at Re=1397

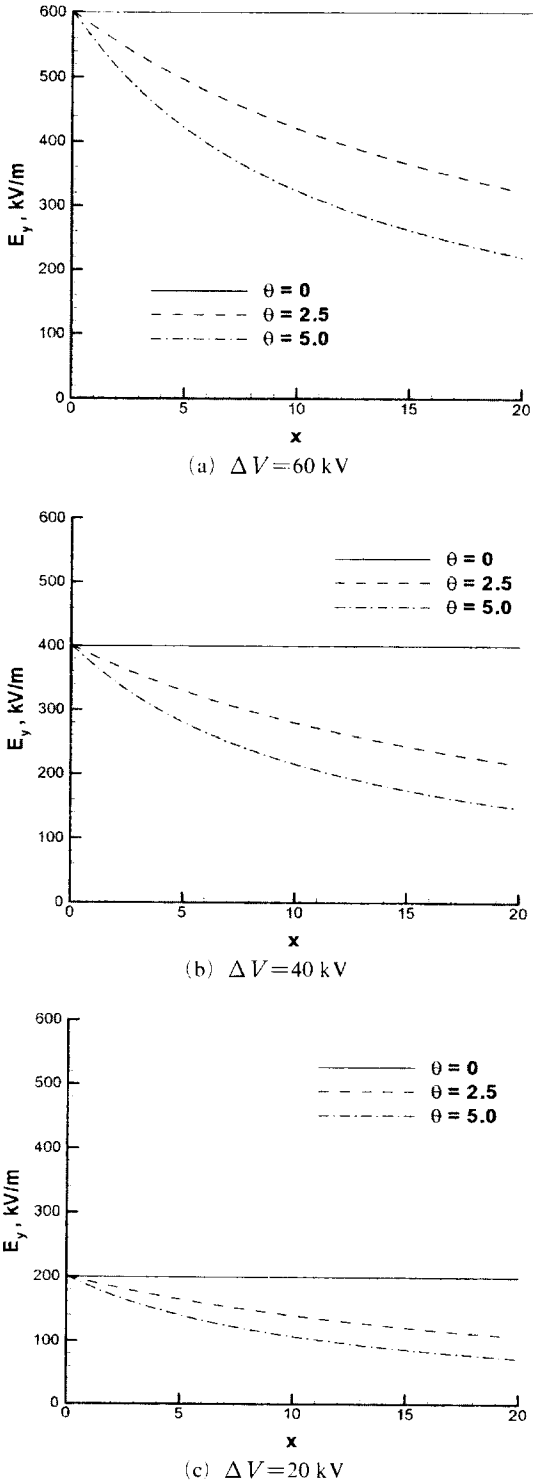

(a) $\Delta V=60$ kV

(b) $\Delta V=40$ kV

(c) $\Delta V=20$ kV

Fig. 5 E_y at the centerline as a function of x for different electrode angles and applied voltage differences

decreasing E_y along the streamwise direction. The y-directional electric field E_y increases with increasing applied voltage difference ΔV, as shown in Fig. 5. This electric field is used to calculate the electrostatic force term, Q, in Eq. (4). Thus, so far as the electrostatic force is concerned for the particle separation, the parallel ESP with $\theta=0$ is better than the inclined ESP with $\theta>0$, because the electrostatic force for the parallel ESP is larger than the inclined one.

The velocity and electric fields shown in Fig. 4 and 5 are used to calculate the particle trajectory and separation efficiency. Table 1 shows the conditions used in the present calculation to simulate the bench scale experiment by Lee and Shin (2001), to separate PVC particles from binary plastic mixtures.

Figure 6 shows the electric charge distribution of negatively charged PVC particles measured in the bench scale experiment. In order to calculate the particle trajectory using the Lagrangian method, we divide the charge distribution of PVC in Fig. 6 equally into 100 parts. The number of particle used in the present calculation is 1000.

Table 1 Conditions used in the present calculation

$Re=140$
$St=9.4\sim150$
$G=1.964$
$Q_{y0}=0.2\sim0.6$

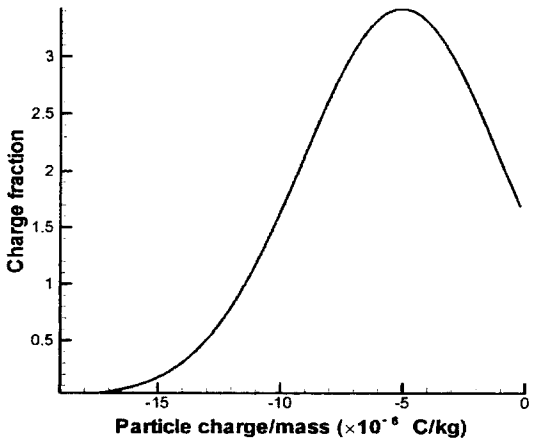

Fig. 6 Electric charge distribution of negatively charged PVC particle

This charged particle is distributed randomly at the nozzle exit using the random number generated in the computer. The particle velocity at the nozzle exit is 70% of the fluid velocity, based on the experimental observation by Lee and Shin (2001). The calculation of particle trajectory is carried out until the negatively charged particle is deposited on the positive electrode surface or escape from the outlet of ESP.

Figure 7 shows the typical trajectory of PVC particle charged negatively for $Re=1397$, $St=150$, $G=1.964$, $Q_0=0.6$ for different angles of $\theta=0°$, 2.5° and 5.0° and for different decay rates of charge after impact. $Q_{y0}\left(=\frac{q_{avg}E_{y0}H}{m_pU^2}\right)$ in Fig. 7 represents the dimensionless parameter for the electrostatic force based on average charge of PVC particle, q_{avg}, and electric field at the inlet of ESP, E_{y0}. In this calculation, it is assumed that, when the particle hits the electrode surface, the particle is rebounded under the perfect elastic collision. In order to consider the effect of the decay rate of electric charge after the particles hit the electrode wall on the particle trajectory, the different decay rates of $\Delta q_{decay}=0\%$, 20%, 50% and 100% are considered in the present study. If the electrostatic force is not present, the particle follows the fluid flow, which is almost parallel to the plane electrodes, and then escapes the outlet of ESP without hitting any electrode surface. However, in the presence of the electrostatic force, the negatively charged particle trajectory deviates from the fluid flow, directs to the positive electrode due to the electrostatic force acted on the y-direction and hits the electrode surface.

Under the perfect elastic collision, the particles are reflected with the same angle and velocity magnitude as the incident ones. If the electric charge does not decay after hitting the wall with $\Delta q_{decay}=0\%$, the particle is still influenced strongly by the electrostatic force acted in the y-direction and directs again to the positive electrode. For the parallel ESP with $\theta=0°$ and $\Delta q_{decay}=0\%$, the location, at which the particle escapes the outlet of ESP, is very close to the positive electrode at $y=-H$. If Δq_{decay} increases to 20% and 50%, the electrostatic force in the y-direction

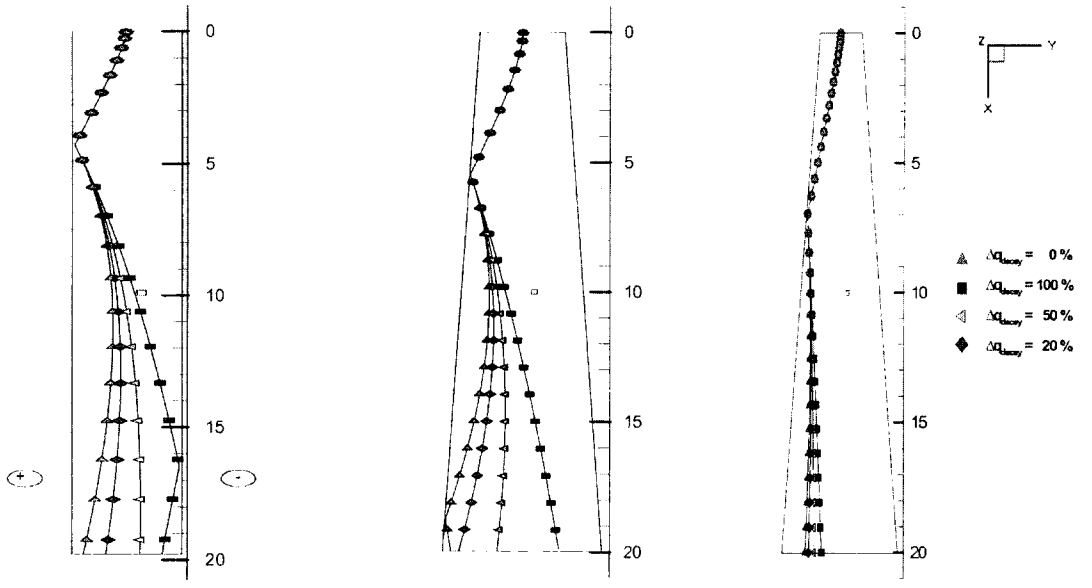

Fig. 7 Trajectory of PVC particle for Re=1397, St=150, G=1.964 and Q_{y0}=0.6 for different angles of θ=0°, 2.5° and 5.0° and for different decay rates of charge after particle impact

decreases because Q in Eq. (4) is linearly proportional to the electric charge q. Thus the distance between the particle at the outlet of ESP and the positive electrode increases with increasing Δq_{decay}. When Δq_{decay}=100% and θ=0°, the particle loses its electric charge fully after it hits the positive electrode. In this case, the electric force acted on the particle does not exist any more and the balance between the drag and gravity force determines the particle trajectory. Thus, when Δq_{decay}=100% and θ=0°, the particle reflected on the positive electrode hits the negative electrode, is rebounded again to the main fluid flow, and then escapes the outlet of the ESP finally, as shown in Fig. 7(a). If the angle of electrodes is increased to 2.5° as shown in Fig. 7 (b), the electric field E_y for 2.5° is less than that for θ=0° as shown in Fig. 5, resulting in decreasing electrostatic force with increasing angle of electrodes. Thus the distance from the inlet to the first deposition position, at which the particle hits the positive electrode, increases with increasing θ. When the particle hits the positive electrode, the incident and reflected angles for θ=2.5° are larger than those for θ=0°. Thus, when the reflected particle moves downstream with Δq_{decay}=0%, the distance between the reflected particle and the positive electrode for θ=2.5° is less than that for θ=0°. The reflected particle from the first deposition location on the positive electrode for θ=2.5° is incident on and reflected from the second position of positive electrode again, which is very close to the outlet of ESP, unlike to the case for θ=0°, before the particle escapes finally the outlet of ESP. Similar to the case for θ=0°, the distance between the particle at the outlet and the positive electrode for θ=2.5° increases with increasing Δq_{decay}. When Δq_{decay}=100% and θ=2.5°, the reflected particle from the first deposition location does not hit the negative electrode any more, unlike to the case for θ=0°, because the distance between the positive and negative electrodes at θ=2.5° is larger than that at θ=0°, as shown in Fig. 7. If the angle of electrodes is increased further to 5°, the electrostatic force keeps decreasing with decreasing electric fields as shown in Fig. 5 and the distance between the positive and negative electrodes keeps increasing, compared to those for θ=0° and 2.5°. Thus the distance from the inlet

to the first deposition location of particles for $\theta=5°$ is larger than that for $\theta=0°$ and 2.5°. All the reflected particles from the positive electrodes escape the outlet without hitting the positive and negative electrodes again. The effect of Δq_{decay} on the position of particle at the outlet of ESP for $\theta=5°$ is relatively smaller, compared to that for $\theta=0°$ and 2.5°, due to the relatively small electrostatic force with increasing angle of electrodes and increasing distance between the electrodes.

Figure 8 shows the deposition fraction of the total number of particles injected into the ESP through the nozzle that is in a certain dimensionless horizontal distance interval or band. The effect of Stokes number and electrode angles on the deposition fraction is considered in Fig. 8. Here the deposition distance x is defined as the location where the negatively charged particle hits the positive electrode first as shown in Fig. 7. When $\theta=0°$ and the electrodes are parallel, the electric field E_y is uniform as shown in Fig. 6 and the electrostatic force is relatively stronger than that for $\theta=2.5°$ and $\theta=5°$. Thus, in the range of Stokes number of 9.4~150 at $\theta=0°$, the electrostatic force acted in the y-direction is greater than the drag force in the same direction. The effect of Stokes number on the particle deposition is not large and the deposition occurs mainly around $6<x<6.8$ when $\theta=0°$, as shown at the upper part in Fig. 8. If the angle of electrodes is increased to 2.5° and 5°, the electric field E_y and electrostatic force decrease significantly, compared to that $\theta=0°$. Thus the distance from the inlet to the particle deposition (first hitting position) on the positive electrode increases with increasing θ, as shown in Fig. 7 and 8. The inertia force acted on the particle in Eq. (4) increases with increasing Stokes number, resulting in increasing deposition distance. Thus the effect of Stokes number on the particle deposition distance at 2.5° and 5° becomes larger, compared to the small effect of Stokes number at $\theta=0°$, because the electrostatic force decreases with increasing θ.

Figure 9 shows the deposition fraction as a function of streamwise distance x for different electrostatic forces and electrode angles at Re=

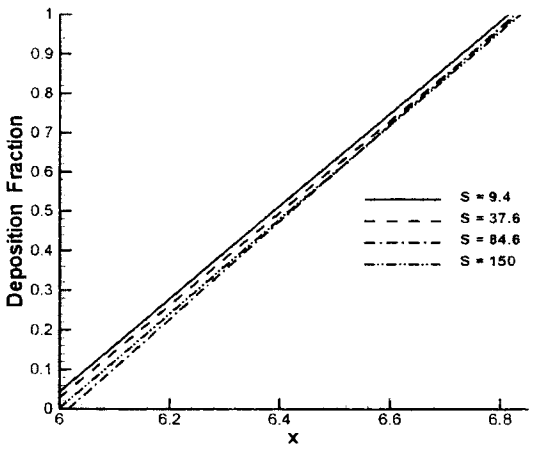

(a) $\theta=0°$

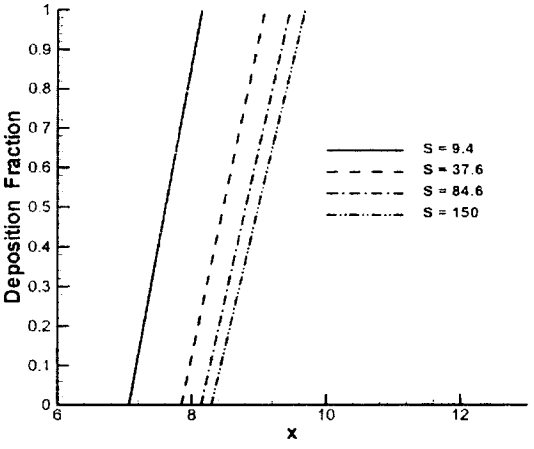

(b) $\theta=2.5°$

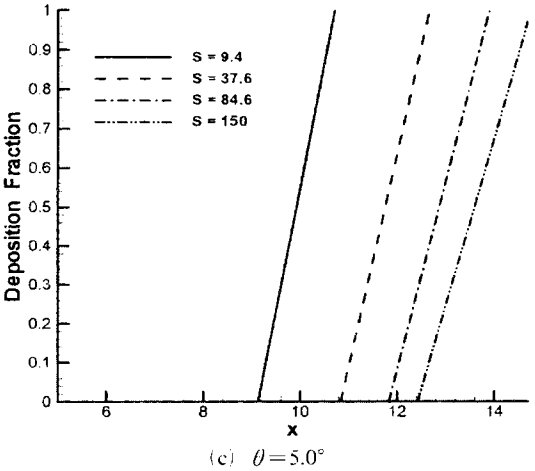

(c) $\theta=5.0°$

Fig. 8 Deposition fraction as a function of x for different electrode angles and stokes numbers at Re=1397 and $Q_{y0}=0.4$

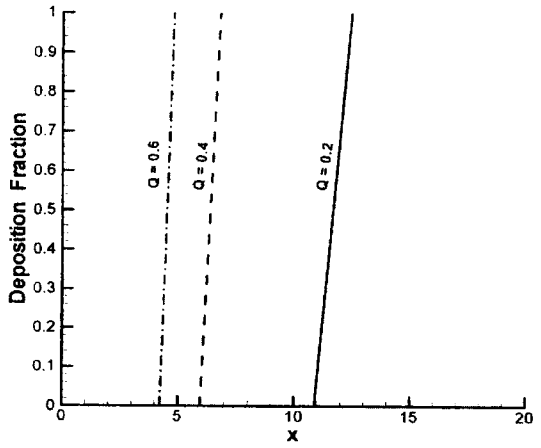

(a) $\theta=0°$

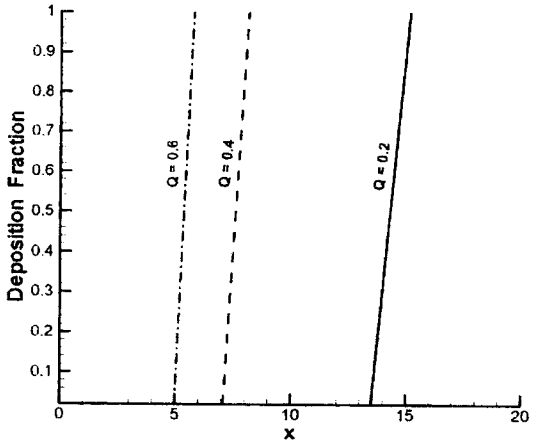

(b) $\theta=2.5°$

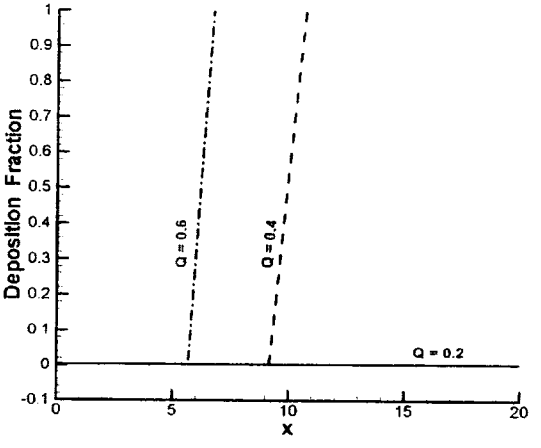

(c) $\theta=5.0°$

Fig. 9 Deposition fraction as a function of x for different electrode angles and $St=9.4$ at Re=1397

1397, $St=9.4$. When $Q_{y0}=0.2$ and $\theta=0°$, the particle deposition distance from the inlet is about 11.1~12.5. If Q_{y0} is increased to 0.4 and 0.6, the particle deposition distance decreases to about 6.05~6.85 and 4.26~4.82, respectively, due to increasing electrostatic force acted on the particle. This result shows that the deposition distance is approximately inversely proportional to Q_{y0}. If the angle of electrodes is increased to 2.5°, the general trend for the deposition distance for different Q_{y0} is similar to the case for $\theta=0°$, resulting in the decreasing deposition distance with increasing Q_{y0}. However, the deposition distance for $\theta=2.5°$ is larger than that for $\theta=0°$, due to decreasing electrostatic force distribution in the ESP with decreasing E_y. When the angle of electrodes is increased to 5° and $Q_{y0}=0.2$, the particle escapes the outlet of ESP without hitting the positive electrodes, resulting in the zero deposition fraction on the positive electrode, because the electric fields and electrostatic force distribution in the ESP is small. If Q_{y0} is increased to 0.4 and 0.6 at $\theta=5°$, the particle hits the positive electrode and the deposition distance decreases with increasing Q_{y0} from 0.4 to 0.6, similar to the cases at $\theta=0°$ and 2.5°.

Figure 10 shows the deposition fraction along the streamwise direction for different electrode angles at Re=1397, St=9.4, and $Q_{y0}=0.4$, to show the effect of electrode angle on the particle

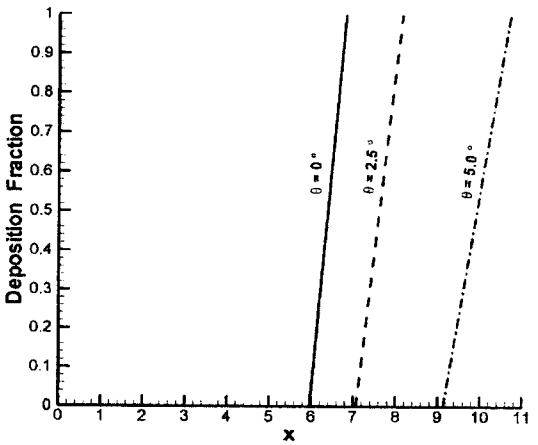

Fig. 10 Deposition fraction as a function of x at Re=1397, $St=9.4$ and $Q_{y0}=0.4$

deposition more clearly. As explained in Fig. 8 and 9, the deposition distance increases due to decreasing electrostatic force acted on the particle with increasing electrode angle. So far as the particle deposition distance (the first hitting position) on the positive electrode is concerned, the parallel ESP at $\theta=0°$ is better than the inclined ESP at $\theta=2.5°$ and 5°, because the electrostatic force field at $\theta=0°$ is stronger in the total region of ESP than that at $\theta=2.5°$ and 5°. However, as shown in Fig. 7, the particle incident on the positive electrode is reflected and the reflected particle velocity depends on the surface conditions of electrode. In this case, the inclined ESP is better than the parallel one, to achieve the goal to separate the particle into the same chemical components. Thus we need to carry out the calculation to consider the effects of both the electric field distribution in the ESP and the rebounding characteristics of particle on the electrode surface to determine the optimal geometry of ESP.

Figure 11 shows the cumulative yield as a function of bin number for $\theta=0°$ and 5° at Re=1397, and $Q_{y0}=0.6$. The quality and effectiveness of the electrostatic separation process can be described by the yield defined as

$$Yield=\frac{Mass\ of\ the\ sought\ component\ in\ the\ extracted\ fraction(s)}{Mass\ of\ the\ processed\ mixture} \quad (12)$$

where PVC yield in bin #1 is described by the ratio of PVC mass collected in bin #1 by PVC mass collected in bins #1-#5. Thus the cumulative yield of PVC in bin #2 can be obtained from the ratio of PVC mass in two bins #1 and #2 divided by the supplied PVC total mass. The predicted yield at the bin #1 for $\theta=0°$ and 2.5° is 95.6% and 90.2%, respectively, showing that the present ESP separate the negatively charged PVC particle from the binary mixtures well. When Re=1397, $St=9.4$, and $Q_{y0}=0.6$, the parallel ESP at $\theta=0°$ is better than the inclined ESP in the view point of PVC particle separation. The present predicted results represent very well the experimental ones given by Lee and Shin (2001), showing that the present results can be used to determine the optimal conditions in the ESP design.

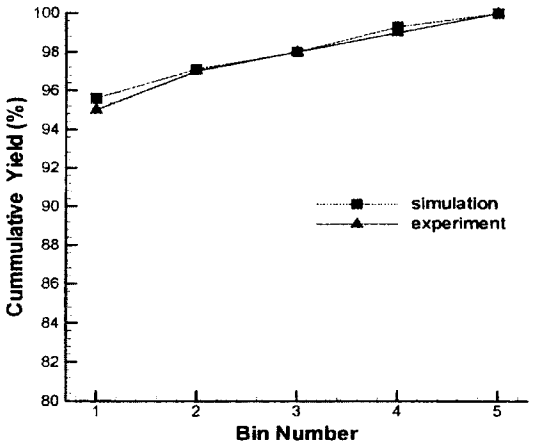

(a) $\theta=0°$

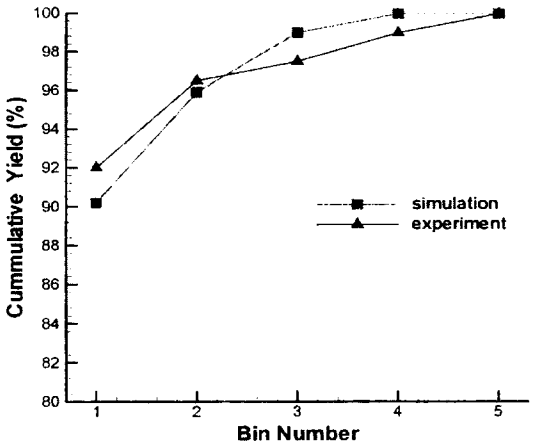

(b) $\theta=5.0°$

Fig. 11 Cumulative yield as a function of bin number for $\theta=0°$ and 5.0° at Re=1397 and $Q_{y0}=0.6$

4. Summary and Conclusions

(1) The fluid flow and electric fields in the precipitator are obtained from the numerical solution of finite volume method. The particle trajectory is obtained using the Lagrangian method.

(2) The effects of electrode angles, electric charge and field distribution, particle size, rebounding on the electrode surface, decay of electric after the impact on the particle deposition and separation are investigated.

(3) So far as the electrostatic force is concerned, the parallel ESP is better than the inclined ESP, because the electrostatic force in the parallel

ESP is larger than that in the inclined ESP. However, so far as the rebounding effect on the electrode surface is concerned, the inclined ESP is better than the parallel one.

(4) The predicted results for the cumulative yield represent very well the experimental one, showing that the present calculation can be used to determine the optimal condition in the ESP design.

Acknowledgment

This study is partially supported by the NRL project.

References

Asano, K., Yatsuzuka, K. and Higashiyama, Y., 1974, "The Motion of Metal Particles within Parallel and Tilted Electrodes," *Journal of Electrostatics*, Vol. 30, pp. 65~74.

Chen, R. Y., Chen, W. C. and Lai, C. S., 1993, "Deposition of Charged Particles in a Channel," *Power technology*, Vol. 74, pp. 135~140.

Chen, R. Y., Chiou, H. C. and Sun, D., 1996, "Deposition of Particles in a Convergent Channel," *Power technology*, Vol. 87, pp. 83~86.

Goo, J. H. and Lee, J. W., 1996, "Monte-Carlo Simulation of Turbulent Deposition of Charged Particles in a Plate-Plate Electrostatic Precipitator," *Aerosol Science and Technology*, Vol. 25, pp. 31~45.

Harper, W. R., 1967, "Contact and Frictional Electrification," Clarendon Press, Oxford.

Inculet, I. I., Castle, G. S. P. and Brown, J. D., 1994, "Tribo-Electrification System for Electrostatic Separation of Plastics," IEEE-IAS Annual Conference Proceedings, Vol. 1, pp. 1397~1399.

Kang, Y., Woo, K. J., Ko, M. H., Cho, Y. J. and Kim, S. D., 1999, "Particle Flow Behavior in Three-Phase Fluidized Beds," Korean J. Chem. Eng., Vol. 16, No. 6, pp. 784~788.

Lu, W. M., Ju, S. P., Tung, K. L. and Lu, Y. C., 1999, "Stability Analysis of Perforated Type Single Stage Suspension Fluidized Bed Without Downcomer," Korean J. Chem. Eng., Vol. 16, No. 6, pp. 810~817.

Lee, J. and Shin, J., 2001, "Triboelectrostatic Separation of PVC Materials from Mixed Plastics for Waste Recycling," Korean J. Chem. Eng., Vol. 19, No. 2, pp. 267~272.

Matsushita, Y., Mori, N. and Sometani, T., 1999, "Electrostatic Separation of Plastics by Friction Mixer with Rotary Blades," *Electrical Engineering in Japan*, Vol. 127, pp. 33~39.

Pearse, M. J. and Hickey, T. J., 1978, "The Separation of Mixed Plastics Using a Dry, Triboelectric Technique," Resource Recovery and Conservation, Vol. 3, pp. 179~190.

Patankar, S. V., 1980, "Numerical Heat Transfer and Fluid Flow," 1st edition, Hemisphere Publishing Co.

Soltani, M., Ahmadi, A., Ounis, H. and McLaughlin, J. B., 1998, "Direct Simulation of Charged Particle Deposition in a Turbulent Flow," Int. J. Multiphase Flow, Vol. 24, No. 1 pp. 77~92.

Takeshita, T., Atsumi, K., Iwasaki, Y. and Harada, T., 1998, "The Triboelectric Separation for Plastic Sheets," J. Soc. Powder Technol., Japan, Vol. 35, pp. 106~110.

Yanar, D. K. and Kwetkus, B. A., 1995, "Electrostatic Separation of Polymer Powders," *Journal of Electrostatics*, Vol. 35, pp. 257~266.